EUROPEAN ORGANIZATION FOR NUCLEAR RSEARCH

CERN PS/87-40 (LPI)

A B S T R A C T

A "Monochromatic" RF Cavity

S. Bartalucci, M. Bell, F. Caspers, K. Hübner, R. Poirier, and A. Susini

The cavity is used in the 600 MeV Electron-Positron Accummulation Ring (EPA) in the LEP injector chain. Nominally, the total beam current is 0.1 A but it can reach 0.3 A for special purposes. The beam is held in 8 bunches (σ_s = 25 cm). The cavity is a capacitively loaded $\lambda/4$ coaxial resonator (L = 1.7 m, D = 0.8 m) operating at 19.1 MHz and providing 50 kV peak voltage. The main cavity volume is in air. In order to control the shunt impedance of the parasitic modes, material becoming very lossy at higher frequencies and, hence, globally damping (up to 40 db) all relevant parasitic modes, is used in the cavity. Ferrite rings with strong magnetic losses at higher frequencies are put close to the gap and a shallow, annular epoxy box filled with circulating tap water surrounds the stem at the short-circuit end of the cavity. Extensive low-level measurements, operating experience and tests with the beam are reported.

Paper presented at the 1987 IEEE Particle Accelerator Conference
Washington D.C., March 16-19, 1987

Geneva, March 1987

CERN PS/87-40
March 1987

A "MONOCHROMATIC" RF-CAVITY

S. Bartalucci, M. Bell, F. Caspers, K. Hübner, P. Marchand, A. Susini

CERN, 1211 Geneva 23, Switzerland

and R. Poirier, TRIUMF, 4004 Wesbrook Mall, Vancouver, B.C., Canada V6T 2A3

1. Introduction

The Electron-Positron-Accumulation ring (EPA) [1] in the LEP injector chain [2] acts as a particle buffer between the fast-cycling (100 Hz) LEP Injector Linac (LIL) and the slow-cycling (0.8 Hz) CERN Proton Synchrotron (CPS). EPA has a circumference of 126m and has operated after start-up in June 1986 at 500 MeV. Only e^- have been stored while e^+ operation is scheduled for March 1987 [1]. The nominal EPA intensities are 2.5 x 10^{10} e^+ and 1.25 x 10^{10} e^- per bunch corresponding to a total current of 76 mA and 38 mA in 8 bunches. However, a current of 240 mA has already been stored. A nominal LIL pulse is 12 ns long but 25 ns is typical. The intensity is $< 3.10^9$/pulse.

In order to have a large longitudinal acceptance the lowest possible harmonic number h = 8 was chosen for EPA yielding f_{rf} = 19 MHz. The maximum r.f. voltage V_{rf} = 50 kV is determined by the momentum acceptance (± 1.2%) of the bucket required by the e^+ LIL pulse. The longitudinal matching to the CPS did not impose further constraints except that adiabatic reduction of V_{rf} to about 10 kV prior to ejection is required if the CPS accelerates with f_{rf}= 7.6 MHz. Since the 8 bunches are closely spaced, parasitic higher modes in the cavity have no time to decay. Therefore, efficient damping of these modes is required. Care was taken that other ring elements would not produce high-Q parasitic resonances.

2. Description of Cavity and Amplifier

As shown schematically in Fig. 1 the cavity is a capacitively loaded λ/4 resonator. The vacuum chamber penetrates into the cavity stem and it crosses the accelerating gap by means of a ceramic cylinder (THOMSON, France). The outer cylinder of the cavity, which must resonate at 19.08 MHz, has a length of 2 m and a diameter of 1 m, and it is made of aluminium, cooled by ambient air. A removable cover allows inspection of the ceramic cylinder and supports. An inflatable r.f. joint provides the necessary continuity along the longitudinal current paths. The choice of the cavity dimensions was governed by the need to have an acceptable R/Q (41 Ω according to SUPERFISH [3]) with a sufficient gap (3 cm) to hold 50kV in air. As a safety precaution, a small pump plus air drier operate continuously to ensure a spark free operation.

The inner conductor consists of a section with low characteristic impedance in form of a thick disc, made of silvered brass, and a 23 cm diameter copper stem. In order to damp parasitic cavity monopole modes, two ferrite rings (TOSHIBA M4C) are placed on both ends of the ceramic cylinder, as proposed by M. Puglisi; they are shielded from the electric field. To improve the damping, an annular water box (30.5 ℓ) is in the cavity at the "cold" end. The box is made from quartz-loaded epoxy and the cover glued onto it has a coned surface on the water side to improve the matching. The damping agent is tap water. In addition, ferrites are placed in the disc and the stem following an idea of Giordano [4]. Radial slits in the disc and longitudinal slits in the stem expose the ferrites to the fields of the cavity dipole modes. In the laboratory, the Q of the accelerating cavity alone without water was measured to be 7340.

For the power amplifier, a Landau-damping cavity from the ISR [5] equipped with a SIEMENS RS 1084 50 kW tetrode, was readapted and magnetically coupled to the accelerating cavity by means of a large lateral port. The anode impedance is controlled by the amount of the anode detuning, which is of the order of 2 MHz. The r.f. voltage was calibrated by means of X-rays observed by a Ge-detector. The level was in agreement with a calibrated probe in the cavity. There are two complementary tuning devices: coarse tuning is obtained by displacing a grounded disc in the gap (sensitivity of 30 kHZ/mm); fine tuning is performed by a plunger at the inductive side with a reduced characteristic of 0.36 kHz/ mm. Since the beam loading is small for the nominal beam current, no beam loading compensation by tuning of the cavity was foreseen. The tuners compensate only slow thermal drifts and so can be simple mechanical ones. The tuning is checked only in the intervals when the beam current is zero by measuring the angle between the grid voltage of the power tube and a signal from a loop in the cavity.

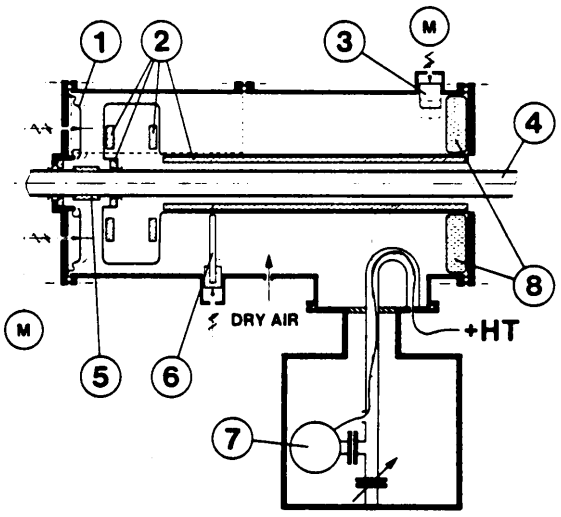

Fig. 1: Cavity Layout; (1) Coarse tuner (2) Ferrite absorbers (3) Fine tuner (4) Vacuum chamber (5) Ceramic cylinder (6) Ceramic Support (7) Power Tube (8) Water Box

3. Damping of Parasitic Cavity Modes

3.1 Threshold Calculations - A laboratory model of the cavity was soon available for measurements. The dimensions were nearly identical to the final cavity but the amplifier cavity was not coupled to it. The monopole (no ϕ dependence) and the dipole cavity modes (sin ϕ dependence) were calculated with URMEL [6]. Table I gives the lowest cavity monopole modes. The shunt impedance R_s is defined by $(V/T)^2/2P$.

In order to avoid longitudinal coupled-bunch oscillations, the maximum admissible shunt impedance R_{smax} was calculated as function of frequency. It is obtained by setting the growth-rate of the instability [7] equal to the longitudinal radiation damping rate m/τ_ε for the worst case when the beam coupled-bunch mode frequency is exactly identical to the

Table I, Cavity monopole modes

f_r (MHz)	R_s/Q (Ω)	Q_{calc} /10^3	Q_{max} /10^3
19	34.8	9.25	-
97	1.3	18.31	0.18
202	1.2	22.87	0.16
270	9.2	11.42	0.03
322	1.7	27.53	0.19
405	0.8	31.45	0.68
469	6.8	17.27	0.13
493	2.9	23.59	0.35

frequency of a cavity monopole mode. Fig. 2 shows the result [8] for the nominal current, V_{rf} = 50 kV and sinusoidal modes [9]. Using Fig. 2 and the computed R_s/Q, the maximum admissible Q_{max} shown in Table I was calculated. The same procedure [8] was applied to the dipole cavity modes which could give rise to transverse coupled-bunch modes. It turned out that the R_s of those cavity modes is insufficient for driving the instability even if the modes had the theoretical Q values. Although the real Q-values were expected to be somewhat below the theoretical values, the ratios Q_{calc}/Q_{max} of the monopole modes shown in Table I are so large that it was decided to foresee a reduction of the quality factors by appropriate means in the cavity. This precaution would alleviate the task of a feed-back system which would be installed if the damping in the cavity turned out to be not sufficient or, for later, when a beam current exceeding the nominal value is desired.

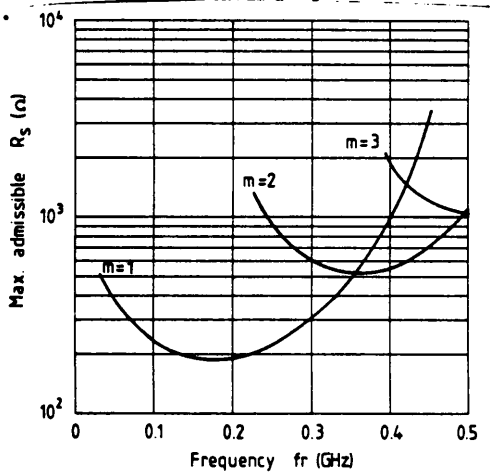

Fig. 2: R_{smax} versus parasitic resonator frequency f_r; m mode number of long. bunch-shape modes

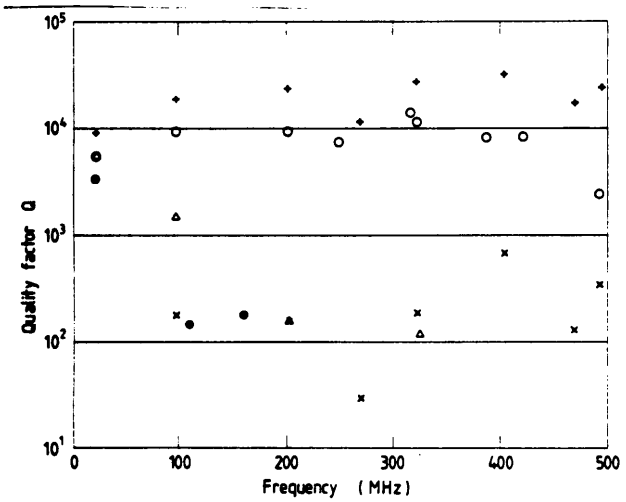

Fig. 3: Q versus f_r; + calcul., x maximum admissible; model cavity: O measured (no damping), Δ measured (1 ferrite ring in); final cavity: • measured.

3.2 Damping of cavity modes - Since damping of so many modes by individually tuned external damping circuits coupled to the cavity by loops or antennae, appeared to be rather complicated, it was preferred to take advantage of the fact that the main cavity volume is in air and to install material which would affect globally all cavity modes without having too adverse effects on the fundamental.

Two possible approaches were tested: ferrite rings close to the gap, which have still very low losses at 19 MHz; an annular water volume around the stem at the side opposite to the gap (Fig. 1), where the electric field of the fundamental is very low but the field of higher modes is already substantial. The dielectric losses in water increasing with frequency damp then mainly the higher modes. As an additional precaution against cavity dipole modes ferrites were foreseen in stem and disc as shown in Fig. 1.

3.3 Measurements [10,11] - The signal transmission between two antennae sticking at two different places into the cavity was measured versus frequency with a HEWLETT-PACKARD 8505 A network analyzer. The Q values were determined from the - 3 db points of the resonance curve. The loading of the modes by the probes was kept at such a low level that the reflected signal from each probe was ≤ 0.1 db. The exciting antenna was always located on the cavity axis in the exit beam hole at the gap; the detecting probe could be introduced into one of the nine holes located at various z, φ coordinates on the outer cylinder of the cavity. Discrimination between monopole and dipoles modes was done: i) by choosing the detecting probe position where the E-field of the mode under investigation was a maximum; inspection of the URMEL field plots allowed us to find these optimum positions; ii) by checking whether the transmission is independent of the φ-position of the detecting probe; iii) by replacing the exciting probe by two symmetric off-axis antennae and by comparison of the transmission for these antennae excited in common and in push-pull mode. Some of the Q measurements were checked with a HEWLETT-PACKARD 8405 A vector voltmeter, which is a convenient method when the resonance frequencies are known.

Fig. 3 gives a plot of Q values of the model cavity calculated by URMEL and the corresponding admissible Q_{max} (cf. Table I). The measured Q-values refer to the case of no damping material present in the cavity and to the case of only one ferrite ring mounted near the gap. In the latter case the ferrites in disc and stem were in. They alone were found to reduce the Q-values between 10 and 80% depending on the mode but have no effect on the fundamental. It is obvious that the damping of the ferrite ring dominated and was appreciable. Not all the original modes could be found. The Q of the 19 MHz resonance was lowered by about 1%, this being the limit of the resolution.

The final cavity is now equipped with two ferrite rings near the gap and an annular water container (see point 2). The addition of the amplifier plus its cavity lowered to Q from 7340 to 5230 with the container empty in both cases. Filling the container with demineralized water lowered the Q to 4920, whereas tap water produced a drop in Q to 3440. As expected, the tap water (tan δ = 0.64 at 20 MHz) was much more efficient in damping than the demineralized water (tan δ = 0.005) [11]. The already existing amplifier could easily cope with the losses in the tap water (3 kW). Since the cooling is no problem and since the high dissipation does away with the need for beam loading compensation by tuning up to the nominal current (beam power loss 0.6 kW), tap water is used at present. Fig. 3 also shows the result of Q measure-

ments done with the final cavity and the amplifier coupled to it but not operating. Only the three lowest modes are still measurable, the other resonances degenerated into broad humps. Their frequencies deviate from the computed values due to the different geometry and the strong damping. Although the R/Q of these modes has not been measured, because no time was available to do perturbation measurements, analogy with the modes of the model cavity suggests that these Q-values are acceptable.

4. Operational experience

The operation of the r.f. cavity has been smooth and reliable on the whole. The design gap voltage of 50 kV is immediately reached even at large tuning angles and no instability has been observed during operation. The tetrode did not display any limitation upon the maximum power that can be applied to the cavity even at the lowest operating gap voltage of 10 kV. The operation of the mechanical tuners, which is fully automatized, proved also to be very good.

The beam-cavity interaction was studied in various conditions to look for possible instabilities and limitations upon the maximum beam current. In particular, the behaviour of the system under beam loading was investigated with the amplitude control loop (AVC) operating and in the special case of no control loop at all. The AVC loop keeps the gap voltage constant in amplitude at a preset value, independent of beam loading and temperature drifts in the cavity.

Some examples of such studies are shown in Fig. 4, where the stability limits are plotted versus the loading phase angle ϕ_L, which is the impedance phase angle as seen by the power generator. For no beam load it is equal to the tuning phase angle ϕ_Z, which is constant in the cases above. The shaded area shows the classical Robinson stability limits that are valid only in the case of no loops. The small change in the synchronous phase ϕ_S with the cavity voltage is not taken into account in Fig. 4. The observed instabilities display a non-oscillatory, pure exponential growth and occur well below the expected thresholds. As the Robinson criterion only applies to a simple parallel resonant circuit model of the r.f. cavity a more sophisticated analysis is in progress to get a better understanding of the observed thresholds. The same holds true for the case of AVC loop, which shows a systematic instability whenever the loading angle crosses the 0° value. These limits are even lower than in the case of no loops, so that a beam loading compensation system is required to substantially improve the machine performances. In Fig. 4 the big dot shows the beam current achieved with the mechanical tuners operated at a higher (by a factor of ≈ 30) sampling rate of the phase error and with nominal accumulation rate. This limit was not due to beam loading but to saturation of accumulation. Although the tuners were not fast enough to keep the ϕ_L constant, the improvement is rather impressive.

To avoid mechanically complicated fast tuners, it was decided to build a feedback acting on the r.f. power amplifier. This loop would automatically keep the cavity voltage constant not only in amplitude but also in phase, thereby providing a fast compensation system. This work is still in progress.

No beam loss could be detected when an electron beam ($N = 3.3 \cdot 10^{11}$; 8 bunches) was reduced to half by ejecting every other bunch. No coupled-bunch oscillations are discernible at nominal intensity at 500 MeV but longitudinal modes appear at 20% higher intensity. Only the mode m = 1 is seen with n depending on the cavity tuning being a hint that the cavity might be the offending element [12]. The strong energy dependence of the criterion described under point 3.1 makes it plausible that the instability threshold will be much higher at 600 MeV.

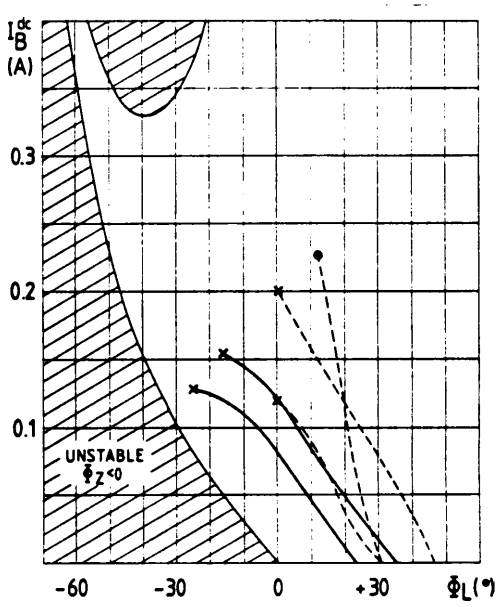

Fig. 4: Stability versus loading angle; a) solid lines, without AVC, b) dashed lines with AVC, c) x measured instability limits, d) • saturation, no instability

Acknowledgements

The authors are grateful to P. Gourcy for the major part of the mechanical and electrical construction of the cavity, to H. Broere for the controls of the tuners and to G. Roubaud for calibrating the gap voltage with X-rays. We also thank R. Garoby for discussions and help during running-in.

References

[1] J.H.B. Madsen et al., Proc. of this Conf.

[2] The LEP Injector Study Group, IEEE Trans. Nucl. Sci. NS-30 (1983) 2022

[3] K.Halbach and R.F.Holsinger, Part. Acc. 7 (1976) 213

[4] S.Giordano, IEEE Trans.Nucl.Sci.NS-30 (1983) 3493

[5] H.Frischholz, S.Hansen, A.Hofmann, E. Peschardt, W.Schnell, Proc. Xth Int. Conf. on High En. Acc., Serpukhov (1977) 36

[6] T.Weiland, report DESY M-82-24 (1982)

[7] F.J.Sacherer, IEEE Tr.Nucl.Sci.NS-24 (1977) 1393

[8] K. Hübner, note PS/LPI 84-28 (1984)

[9] F.J. Sacherer, report CERN/PS/BR 77-6 (1977)

[10] M. Bell, F. Caspers, K. Hübner, R. Poirier and A. Susini, Note PS/RF/85-2 (1985)

[11] S.Bartalucci, A.Susini, Note PS/LPI 86-19 (1986)

[12] S.Bartalucci, J.F.Bottollier, R.Cappi, F.Caspers, J.P.Delahaye, B.Frammery, K.Hübner, A. Krusche, A. Poncet, L. Rivkin, Proc. of this Conf.